

Conductance spectroscopy in ferromagnet–superconductor hybrids

T Yu Karminskaya¹, M Yu Kupriyanov^{1,2}, S L Prischepa³ and A A Golubov^{2,4}

¹Skobeltsyn Institute of Nuclear Physics, Lomonosov Moscow State University, Leninskie gory, Moscow 119991, Russian Federation

²Moscow Institute of Physics and Technology, Dolgoprudny, Moscow 141700, Russia

³Belarusian State University of Informatics and Radio Electronics, Minsk, Belarus

⁴Faculty of Science and Technology and MESA+ Institute for Nanotechnology, University of Twente, 7500 AE Enschede, The Netherlands

E-mail: tatiana.karminskaya@gmail.com

Received 9 January 2014, revised 21 April 2014

Accepted for publication 7 May 2014

Published 5 June 2014

Abstract

We present a theoretical model for the proximity effect in F–SFF–F structures (where F is a ferromagnet and S is a superconductor) with non-collinear magnetization vectors in the F-layers and with arbitrary magnitudes of exchange fields. The electrical conductance of these structures is analyzed within the Keldysh–Usadel formalism in the diffusive regime as a function of the misorientation angle between magnetizations of the F-layers and transparencies of the SF and FF interfaces. We show that long-range triplet superconducting correlations manifest themselves either as a zero-bias peak in the case of perfect transparency of the FF interface, or as a two-peak structure in the case of finite transparency. The predicted features may serve as a diagnostic tool for the characterization of interfaces in superconducting hybrid structures.

Keywords: superconducting hybrid structures, conductance, proximity effect, triplet correlations

The investigation of superconducting correlations in superconductor–ferromagnetic (S–F) hybrid structures is currently a subject of active interest. Quite a number of remarkable phenomena were predicted theoretically in these structures [1–31] and have been experimentally verified [32–52]. Moreover, potential applications of SF-based devices as memory elements in superconducting computers have been recently proposed [53–55].

There are several types of spin valve devices that potentially can be used as memory elements [48–52, 56–60]. Among them, only the structure proposed in [56–60] can operate in magnetic fields that do not exceed a few tens of oersted. In these devices, there is only one ferromagnetic film, so only short-range spin triplet correlations are present in such structures. Contrary to that, in other spin valve realizations [48–52] there are several magnetic layers. In these structures, deviations of the relative magnetizations of ferromagnetic films from collinear to non-collinear leads to the generation of long-range triplet superconducting correlations. This process is accompanied by either suppression of the critical temperature [51, 52], T_c , or by changing the sign of the

supercurrent in the triplet pairing channel [48–50]. In both cases, an implementation of these effects requires an application of an external magnetic field of the order of 10^3 Oe. It is obvious that such large magnetic fields cannot be easily combined with the RSFQ circuits.

An alternative is to use structures with long ferromagnetic films, suggested in [23]. The decay length of the long-range triplet superconducting component is insensitive to the magnitude of the exchange field, therefore these correlations penetrate into ferromagnetic material at longer distances. Such correlations can be observed in long ferromagnetic wires in the parts where singlet and short-range triplet correlations are suppressed due to their fast decay in space, intrinsic to materials with a large magnitude of the exchange energy. The long-range triplet correlations can survive in long ferromagnetic films attached to SFF structures in which long-range triplet pairing can nucleate. The presence of these triplet correlations changes the density of states (DoS) in the film, so it must also be accompanied by changes in the conductance of this film due to the proximity effect. It provides an opportunity for the realization of a spin valve in which the external

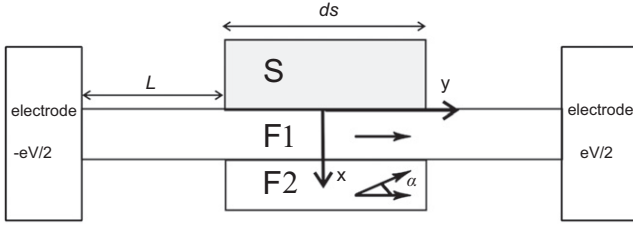


Figure 1. The geometry of the considered F1–SF1F2–F1 structure.

magnetic field controls the magnitude of conductance of a ferromagnetic film.

To evaluate the magnitude of this effect, we analyze a simple model problem below. Namely, we investigate correlations in F1–SF1F2–F1 structures (see figure 1) that represent a long thin ferromagnetic wire, F1, with the length $2L + d_s$. It connects two massive normal electrodes. In its middle part, the F1 layer is in contact with a thick superconducting film, S, located on the top of the wire and a thin ferromagnetic film, F2, placed on the bottom of the wire (the lengths, d_s , of the S and F2 films are identical). The magnetization vector of the long ferromagnetic wire is constant and it is directed along the y -axis. The magnetization vector of the short ferromagnetic film F2 is declined from the first vector on an angle α in the y - z plane, thus providing the conditions for the realization of long-range triplet superconducting correlations in the structure. Here, we present the results of calculations for the DoS and differential conductance along the F1 film in the F1–SF1F2–F1 structure with noncollinear magnetizations of the ferromagnetic layers that also differ with the values of the exchange energies. The calculations are done in the diffusive limit in the framework of the Usadel equations for both linear and nonlinear cases. We present the differential conductance of the F1 film as a function of the angle α . We show that the maximum value of the differential conductance is achieved not at $\alpha = \pi/2$ (as was found in [4] and [29] for the out-of-plane geometry for normal current injection), but at some intermediate angle that depends on the difference between the values of the exchange energy of the F films. We also investigate the influence of the suppression parameter at the F1F2 interface on the shape of the differential conductance.

We will discuss the properties of the structure in the frame of Usadel equations that can be written as:

$$D\nabla(G\nabla G) + i\varepsilon[\hat{k}_0\hat{\tau}_3\hat{\sigma}_0, G] - i[\hat{k}_0\bar{h}, G] = 0, \quad (1)$$

where parameter $\bar{h} = h_2(\hat{\tau}_3\hat{\sigma}_3 \cos \alpha + \hat{\tau}_0\hat{\sigma}_2 \sin \alpha)$ for the F2 layer and $\bar{h} = h_1\hat{\tau}_3\hat{\sigma}_3$ for the F1 film (\hat{k} , $\hat{\tau}$, $\hat{\sigma}$ are 2×2 Pauli matrices in the Keldysh, Nambu–Gorkov and spin spaces correspondingly), h_1 and h_2 are normalized on the πT_C exchange energies of the upper and lower F films, respectively, D is the diffusion coefficient, and ε is a quasiparticle energy. The Green's function, G , is an 8×8

matrix:

$$G = \begin{pmatrix} G^R & G^K \\ 0 & G^A \end{pmatrix}.$$

Here, G^R , G^A , G^K are the retarded, advanced and Keldysh Green's functions, correspondingly. The elements of matrix G^K can be connected by the distribution function $f = f_L\hat{\tau}_0\hat{\sigma}_0 + f_T\hat{\tau}_3\hat{\sigma}_0$ (which is a 4×4 matrix):

$$G^K = G^R f - f G^A. \quad (2)$$

In thermodynamic equilibrium, which in our case is achieved in the electrodes (see figure 1), the distribution function is expressed by

$$f_{L,T} = \frac{1}{2} \left[\tanh\left(\frac{\varepsilon + eV}{2T}\right) \pm \tanh\left(\frac{\varepsilon - eV}{2T}\right) \right], \quad (3)$$

where V is an applied voltage (figure 1). Consequently, it is sufficient to determine only the retarded function. This function can be represented as

$$\begin{aligned} G^R &= \hat{\tau}_3 g + \hat{\tau}_0 g_t + i\hat{\tau}_2 f + \hat{\tau}_1 f_t, \\ f &= \hat{\sigma}_3 f_3 + \hat{\sigma}_0 f_0, f_t = \hat{\sigma}_1 f_1, \\ g &= \hat{\sigma}_0 g_0 + \hat{\sigma}_3 g_3, : g_t = \hat{\sigma}_2 g_2, \end{aligned}$$

where f_3, f_0, f_1 are the condensate Green's functions describing singlet, short-range and long-range triplet correlations; and g_0, g_3, g_2 are normal Green functions, respectively. With these definitions, the normalization condition $G^2 = 1$ transforms to

$$\begin{aligned} g_0^2 + g_3^2 + g_2^2 - f_3^2 - f_0^2 + f_1^2 &= 1, \\ f_1 f_3 + g_2 g_0 &= 0. \end{aligned} \quad (4)$$

Equation (1) must be supplemented by boundary conditions matching Green's functions across the interfaces

$$\gamma_B G_l \frac{\partial}{\partial x} G_l = \pm [G_l, G_r], \quad (5)$$

$$\gamma_F G_l \frac{\partial}{\partial x} G_l = G_r \frac{\partial}{\partial x} G_r. \quad (6)$$

At $y = \pm (L + d_s/2)$

$$G_l = 0, \quad (7)$$

while the electron energy distribution functions are equal to their equilibrium values (3). Here the indices l and r refer to the upper or lower layer with respect to the SF1 and F1F2 boundaries.

The transport properties of both F1F2 and F1S interfaces are characterized by the interface parameters

$$\gamma = \frac{\rho_S \xi_S}{\rho_F \xi_F}, \quad \gamma_B = \frac{R_{BF} \mathcal{A}_B}{\rho_F \xi_F}, \quad \gamma_{BS} = \frac{R_{BS} \mathcal{A}_B}{\rho_F \xi_F}. \quad (8)$$

Here R_{BF} , R_{BS} and \mathcal{A}_B are the resistances and the area of the F1F2 and F1S interfaces, $\xi_{S,F} = (D_{S,F}/2\pi T_C)^{1/2}$ and $D_{S,F}$ are the decay lengths and diffusion coefficients of the S and F materials, while ρ_S and ρ_F are their resistivities.

To simplify the problem, we assume below that the normal state resistivities and coherence lengths of ferromagnetic films are identical ($\gamma = 1$ at the F1F2 interface), and ferromagnetic films are thin. The second assumption allows us to transfer the solution of the problem (1)–(6) to a one-dimensional one (see [22–24] for the details). We also assume that the suppression parameters at the FIS interface satisfy the condition $\gamma \ll \xi_F / (d_F \max(1, \sqrt{h_{1,2}})) + \gamma_{BS}$ allowing us to ignore the suppression of superconductivity in the S electrode (it can be simply achieved from the above boundary conditions). We assume, further, that the length, L , is smaller compared to the characteristic lengths of inelastic scattering inside the F1 layer.

Under the above assumptions, it is possible to derive from (1) the equation for electron energy distribution for a F1–SF1F2–F1 structure in the form of the diffusion equation

$$\frac{\partial}{\partial x} \left(M \frac{\partial}{\partial x} f_T \right) = 0, \\ M = [Reg_0]^2 + [Reg_3]^2 + [Reg_2]^2 + [Imf_3]^2 \\ + [Imf_0]^2 + [Ref_1]^2.$$

Integrating this equation with boundary conditions (7) we get an expression for the distribution function f_T and from the general expression for the current

$$I = \frac{1}{2R} \int Tr \sigma_0 \tau_3 \left(G^R \frac{\partial}{\partial y} G^K + G^K \frac{\partial}{\partial y} G^A \right) d\varepsilon \quad (9)$$

and (2) we arrive at

$$I = \frac{d}{R} \int_0^\infty \frac{2f_T}{\int_{-d}^d \frac{dy}{M}} d\varepsilon, \quad (10)$$

where $d = L + d_s/2$ and R is the resistance of the ferromagnetic layer.

In the limit of zero temperature from (10) for the normalized differential conductance $\sigma(V) = R dI/dV$ of a long ferromagnetic film in the direction along the F1F2 interface, we have

$$\sigma = \frac{2d}{\int_{-d}^d \frac{dy}{[Reg_0]^2 + [Reg_3]^2 + [Reg_2]^2 + [Imf_3]^2 + [Imf_0]^2 + [Ref_1]^2}}. \quad (11)$$

Expression (11) can be simplified in the linearized case when the suppression parameter γ_{BS} is large enough. In this limit, the superconductivity induced into the F1 wire is small and in the zero approximation $g_0 = 1$, $g_{3,2} = 0$. Taking into account the normalization condition (4), we can express g_0 through the other functions in the next approximation and transform expression (11) to:

$$\sigma = \frac{2d}{\int_{-d}^d \frac{dy}{1 + [Ref_3]^2 + [Ref_0]^2 + [Imf_1]^2}}. \quad (12)$$

Note that the expression for differential conductance similar to equation (12) was obtained for an SNN structure ($Ref_0 = 0$, $Imf_1 = 0$) in [61]. The conductance in superconducting hybrids in a similar T-shaped geometry was further studied in [62, 63] (see the review in [64]) and in [65]. However, in the structures considered in [62–64], no ferromagnetic layers were attached, and therefore there were no odd superconducting correlations. In the structure considered in [65], there also were no ferromagnetic layers, but odd triplet correlations were generated due to the proximity effect between a p-wave superconductor and a diffusive N-layer.

We start our analysis of processes in the F1–SF1F2–F1 structure by considering the case of a transparent F1F2 interface ($\gamma_{BM} = \gamma_B d_F / \xi_F = 0$.) This limiting case is simple. However, it reveals the main effects without any distortion due to the influence of the F1F2 interface. In the linearized case, analytical solutions of the problem ((1)–(7)) for condensate functions f_3, f_0, f_1 in the free part of the upper F film can be easily derived:

$$f_1 = \Gamma \frac{h_2 \sin(\alpha) \frac{\sinh(q(d-y))}{\sinh(q(d-d_s/2))}}{h_1^2 + h_2^2 + 2h_1 h_2 \cos(\alpha) - 4e^2}, \quad (13)$$

$$f_0 = i \frac{\Gamma \sum_{j=1,2} \frac{[(-1)^{j+1} 2e + h_1 + h_2 \cos(\alpha)] \sinh(q_j(d-y))}{\sinh(q_j(d-d_s/2))}}{2 \frac{h_1^2 + h_2^2 + 2h_1 h_2 \cos(\alpha) - 4e^2}}, \quad (14)$$

$$f_3 = i \frac{\Gamma \sum_{j=1,2} \frac{[2e + (-1)^{j+1} (h_1 + h_2 \cos(\alpha))] \sinh(q_j(d-y))}{\sinh(q_j(d-d_s/2))}}{2 \frac{h_1^2 + h_2^2 + 2h_1 h_2 \cos(\alpha) - 4e^2}}. \quad (15)$$

In these expressions, $q = \sqrt{-i\varepsilon}$, $q_{1,2} = \sqrt{-i\varepsilon \pm ih_{1,2}}$ and $\Gamma = \Delta / (\gamma_{BMS} \sqrt{\varepsilon^2 - \Delta^2})$, where Δ is the modulus of the order parameter of the superconductor, and $\gamma_{BMS} = \gamma_{BS} d_F / \xi_F$. It is necessary to note that to get (13)–(15), we also neglect the suppression of the Green's functions in the part of the F1 film located under the superconductor due to the proximity effect and use the rigid boundary conditions at $x = \pm d_s/2$.

Figure 2 shows the dependence of the correction to the differential conductance ($\delta\sigma = \sigma - 1$) normalized to the conductance in the normal state as a function of the misorientation angle α calculated at zero voltage from (12)–(15) for three different lengths of the long ferromagnetic film ($L/\xi_F = 1$, $L/\xi_F = 5$, $L/\xi_F = 30$). Here, we consider that the exchange energies of the two F films are different ($h_1 = 2$, $h_2 = 5$). Note that at $h_1 = h_2$, the conditions of the linear approximation are violated at zero voltage.

For the short upper ferromagnetic film ($L/\xi_F = 1$), the conductance rises from $\alpha = 0$ to $\alpha = \pi$ monotonically since all correlations are still present in the structure, and the magnetic configuration for $\alpha = \pi$ corresponds to a smaller average exchange energy in comparison with $\alpha = 0$. It is also seen from the figure that the shape of the $\delta\sigma$ dependencies begins to change with the increase in L . The reason for this

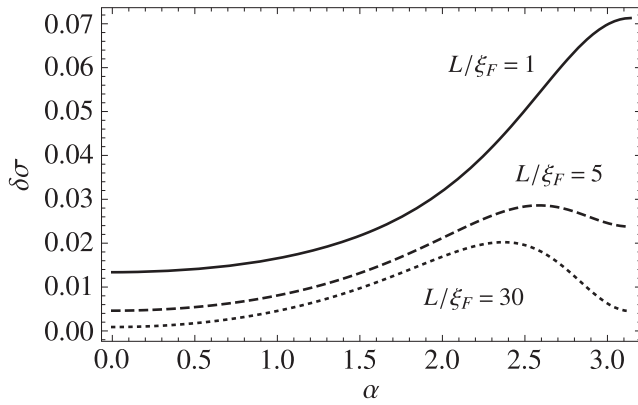


Figure 2. The correction to conductance, $\delta\sigma$, vs the angle between the magnetization vectors, α , in the case of a large value of the parameter γ_{BS} for $V = 0$ and $T = 0$ at $h_1 = 2$, $h_2 = 5$, for $L/\xi_F = 1$ (solid line), $L/\xi_F = 5$ (dashed line) and $L/\xi_F = 30$ (dotted line).

transformation is that singlet and short-range triplet components begin to decrease very quickly deep into the long parts of the upper F film in comparison with the long-range triplet part that decreases slowly. For $L/\xi_F = 30$ (the dotted line in figure 2), as well as in a limit of the long upper ferromagnetic film, $L \gg \xi_F$, only these long-range triplet correlations can be taken into account. Expressions (12)–(14) give, in this case,

$$\sigma = 1 + \left(\frac{h_2 \sin(\alpha)/\gamma_{BS}}{h_1^2 + h_2^2 + 2h_1h_2 \cos(\alpha)} \right)^2. \quad (16)$$

It is seen that in the vicinity of the angles $\alpha = 0$ and $\alpha = \pi$, the correction to the conductivity is negligible. This is a consequence of the fact that at these angles there are no long-range triplet correlations in the structure.

The dependence of the differential conductance has a maximum at some intermediate angle

$$\alpha_m = \arccos \left(\frac{-2h_1h_2}{h_1^2 + h_2^2} \right).$$

It is seen that the position of the maximum is the function of the exchange energies only, and it is always located at $\alpha > \pi/2$ since the exchange energies are different in this case. In the area near α_m , the long-range triplet correlations declare themselves very strongly.

This can also be seen from figure 3. It shows the dependencies of the correction to the differential conductance on the applied voltage for the long upper ferromagnetic film $L/\xi_F = 30$ for three different misorientation angles $\alpha = 0.5$, $\alpha = 2.4$ and $\alpha = \pi$. At zero voltage, there is a strong peak in the differential conductance at $\alpha = 2.4$. It is exactly the angle at which there is the maximum in the $\delta\sigma(\alpha)$ dependence calculated for $V = 0$ (see the dotted line in figure 2). With the inclination of the angle α from α_m , the height of the peak decreases since the influence of the long-range triplet component decreases.

Let us discuss the behavior of the differential conductance beyond the linearized case for an arbitrary value of the parameter γ_{BS} . To calculate it, the nonlinear

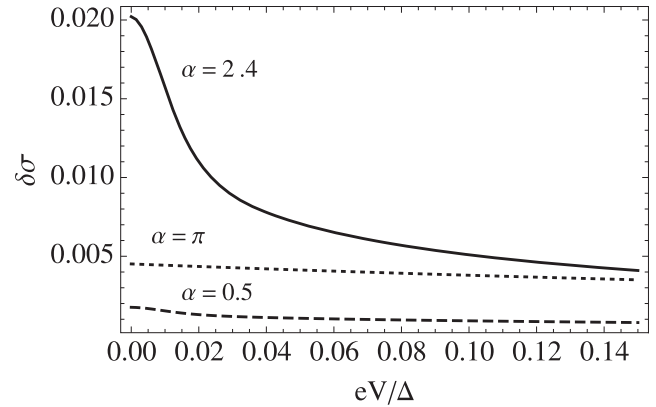


Figure 3. The correction to the conductance, $\delta\sigma$, vs the applied voltage eV/Δ at $h_1 = 2$, $h_2 = 5$, $L/\xi_F = 30$ and $T=0$ for $\alpha = 0.5$ (dashed line), $\alpha = 2.4$ (solid line) and $\alpha = \pi$ (dotted line).

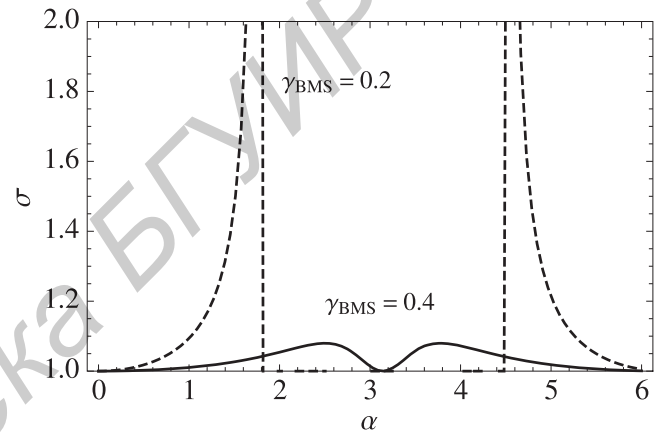


Figure 4. The conductance, σ , vs the angle between the magnetization vectors, α , at zero voltage, $h_1 = 2$, $h_2 = 5$, $L/\xi_F = 30$ for two different values of the parameter γ_{BMS} : $\gamma_{BMS} = 0.2$ (dashed line), $\gamma_{BMS} = 0.4$ (solid line).

equations (1)–(6) were solved numerically using the shooting method.

Figure 4 shows the dependence of the conductance of a long upper ferromagnetic film on the angle α at zero voltage. This conductance is caused by long-range triplet correlations, since for a long ferromagnetic film, $L/\xi_F = 30$, only these correlations are strong enough. At $\gamma_{BMS} = 0.4$, the behavior of the conductance is still similar to that seen in figure 2. As the SF interface becomes more transparent (the suppression parameter γ_{BMS} decreases), the peaks on the graph get higher. Further reduction of the suppression parameter results in the appearance of an angle interval in which the correction to the differential conductance is zero and the peaks on the borders of the interval increase sharply (see the dashed line in figure 4).

The appearance of strong peaks can be understood from figure 5. It shows the dependence of the DoS, $\nu = Re(g_0)$, on the energy, ϵ , calculated numerically for $h_1 = 2$, $h_2 = 5$, $L/\xi_F = 30$, $\gamma_{BMS} = 0.2$ and two values of the misorientation angle between the magnetization vectors $\alpha = \pi$ (solid line)

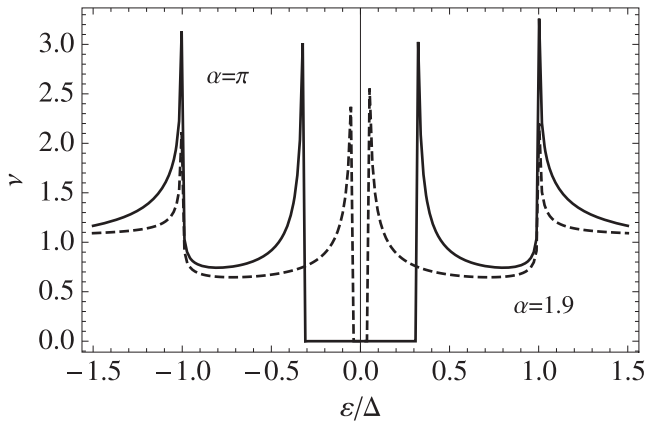


Figure 5. The density of states, ν , vs the energy at zero voltage, $h_1 = 2$, $h_2 = 5$, $L/\xi_F = 30$, $\gamma_{BMS} = 0.2$ for two values of the misorientation angle between the magnetization vectors $\alpha = \pi$ (solid line) and $\alpha = 1.9$ (dashed line).

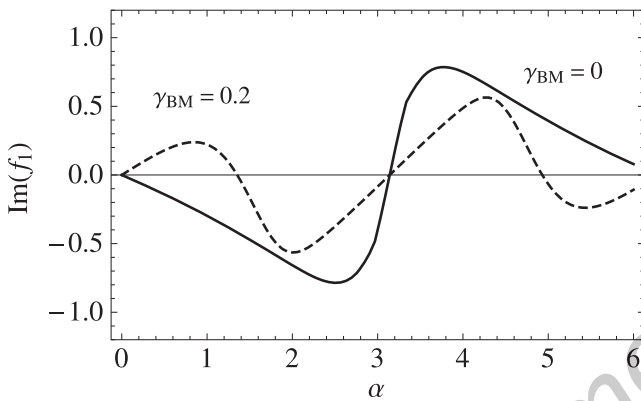


Figure 6. The imaginary part of the equal spin triplet condensate function, f_1 , vs the angle between the magnetization vectors, α , for zero voltage at $h_1 = 2$, $h_2 = 5$, $y = 0$, $\gamma_{BMS} = 0.4$ for two different suppression parameters $\gamma_{BM} = 0$ (solid line) and $\gamma_{BM} = 0.2$ (dashed line).

and $\alpha = 1.9$ (dashed line). At $\alpha = \pi$, there are two peaks in the density of states located at $\varepsilon = \Delta$ and at the position of the minigap. The deviation of the angle α from $\alpha = \pi$ leads to an increase in the effective exchange energy. As a result, the position of the minigap shifts to a smaller energy and there exists an angle α at which the minigap becomes zero and the position of the peak in the density of states is localized at zero energy. It occurs at $\alpha = 1.8$, which is exactly at the angle α at which there are peaks in the dependence $\sigma(\alpha)$ presented in figure 4.

As was discussed earlier in [24] for the SF1F2 structure, the suppression parameter at the F1F2 interface can strongly influence the behavior of long-range triplet correlations leading to an additional phase-slip at the F1F2 interface. Indeed, taking into account the nonzero value of the parameter γ_{BM} at the F1F2 interface, we find that the behavior of the component f_1 in the F1–SF1F2–F1 structure changes significantly (figure 6). The dashed line ($\gamma_{BM} = 0.2$) shows that the triplet component changes its sign at some

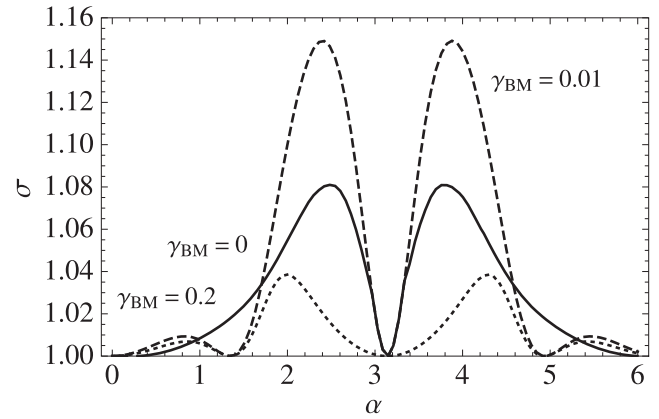


Figure 7. The conductance, σ , vs the angle between the magnetization vectors, α , for zero voltage at $h_1 = 2$, $h_2 = 5$, $L/\xi_F = 30$, $\gamma_{BS} = 0.4$ for two different suppression parameters $\gamma_{BM} = 0$ (solid line), $\gamma_{BM} = 0.01$ (dashed line) and $\gamma_{BM} = 0.2$ (dotted line).

intermediate angle, which is not equal to 0 or π . The magnitude of this angle depends on the difference between h_1 and h_2 and on the suppression parameters γ_{BS} and γ_{BM} . With an increase of the suppression parameters and a decrease of $|h_1 - h_2|$, it moves towards $\alpha = \pi/2$.

Long-range triplet correlations prevail in the long F1 film of the F1–SF1F2–F1 structure, so the features that are seen in figure 6 will remain in the conductance. Figure 7 shows the dependence of the differential conductance of the upper F1 film on the angle α at zero voltage for several values of the suppression parameter $\gamma_{BM} = 0, 0.01, 0.2$. With an increase of γ_{BM} , the shape of the conductance changes due to the changing of the long-range triplet component (the dashed line and dotted lines). In the case of finite transparency of the F1F2 interface, one maximum in differential conductance transforms into two maximums. Also, at $\gamma_{BM} = 0.01$, the maximum value of the conductance (dashed line) can be even larger than for a structure with ideal transparency of the F1F2 interface (solid line). This fact is in good agreement with the discussion performed in [24].

In conclusion, we have investigated the conductance of a long ferromagnetic film in a F1–SF1F2–F1 structure. In the collinear magnetization case, the conductance decreases with the increase in the length of the F1 film (figure 2). However, in the configuration with noncollinear magnetizations, the conductance decreases slowly due to the generation of long-range triplet superconducting correlations. The strong dependence of the differential conductance on the misorientation angle allows us to control the conductance by changing the directions of magnetization of one ferromagnetic film. Furthermore, we demonstrate that long-range triplet correlations manifest themselves as a zero-bias peak in the case of perfect transparency of the F1F2 interface, while a two-peak structure is realized in the case of finite transparency. These features may serve as a diagnostic tool for the characterization of interfaces in superconducting hybrid structures.

Acknowledgments

This work is supported in part by Russian and Belarusian Funds for Basic Research under RFBR-BFBR grants no. 14-02-90018 (MYK) and no. F12R-014 (SLP), EU–Japan collaboration program ‘IRON SEA’ and by the Ministry of Education and Science of the Russian Federation, grant no. 14Y26.31.0007.

References

- [1] Bulaevskii L N, Kuzii V V and Sobyenin A A 1977 *Pis'ma Zh. Eksp. Teor. Fiz.* **25** 314
- [2] Buzdin A I, Bulaevskii L N and Panyukov S V 1982 *Pis'ma Zh. Eksp. Teor. Fiz.* **35** 147
- [3] Buzdin A I and Kupriyanov M Y 1991 *Pis'ma Zh. Eksp. Teor. Fiz.* **53** 308
- [4] Bergeret F S, Volkov A F and Efetov K B 2001 *Phys. Rev. Lett.* **86** 4096
- [5] Kadigrobov A, Shekhter R I and Jonson M 2001 *Europhys. Lett.* **54** 394
- [6] Volkov A F, Bergeret F S and Efetov K B 2003 *Phys. Rev. Lett.* **90** 117006
- [7] Bergeret F S, Volkov A F and Efetov K B 2003 *Phys. Rev. B* **68** 064513
- [8] Volkov A F, Fominov Y V and Efetov K B 2005 *Phys. Rev. B* **72** 184504
- [9] Bergeret F S, Volkov A F and Efetov K B 2005 *Rev. Mod. Phys.* **77** 1321
- [10] Buzdin A I 2005 *Rev. Mod. Phys.* **77** 935
- [11] Golubov A A, Kupriyanov M Y and Il'ichev E 2004 *Rev. Mod. Phys.* **76** 411
- [12] Volkov A F and Efetov K B 2010 *Phys. Rev. B* **81** 144522
- [13] Trifunovic L and Radovic Z 2010 *Phys. Rev. B* **82** 020505
- [14] Houzet M and Buzdin A I 2007 *Phys. Rev. B* **76** 060504
- [15] Eschrig M, Kopu J, Cuevas J C and Schoen G 2003 *Phys. Rev. Lett.* **90** 137003
- [16] Loefwander T, Champel T, Durst J and Eschrig M 2005 *Phys. Rev. Lett.* **95** 187003
- [17] Eschrig M and Loefwander T 2008 *Nat. Phys.* **4** 138
- [18] Eschrig M 2011 *Phys. Today* **64** 43
- [19] Braude V and Nazarov Y V 2007 *Phys. Rev. Lett.* **98** 077003
- [20] Asano Y, Tanaka Y and Golubov A A 2007 *Phys. Rev. Lett.* **98** 107002
- [21] Asano Y, Sawa Y, Tanaka Y and Golubov A A 2007 *Phys. Rev. B* **76** 224525
- [22] Karminskaya T Y and Kupriyanov M Y 2007 *Pis'ma Zh. Eksp. Teor. Fiz.* **86** 65
Karminskaya T Y and Kupriyanov M Y 2007 *JETP Lett.* **86** 61 (Engl. transl.)
- [23] Karminskaya T Y, Kupriyanov M Y and Golubov A A 2008 *Pis'ma Zh. Eksp. Teor. Fiz.* **87** 657
Karminskaya T Y, Kupriyanov M Y and Golubov A A 2008 *JETP Lett.* **87** 570 (Engl. transl.)
- [24] Karminskaya T Y, Golubov A A and Kupriyanov M Y 2011 *Phys. Rev. B* **84** 064531
- [25] Beri B, Kupferschmidt J N, Beenakker C W J and Brouwer P W 2009 *Phys. Rev. B* **79** 024517
- [26] Kupferschmidt J N and Brouwer P W 2011 *Phys. Rev. B* **83** 014512
- [27] Fominov Y V, Golubov A A and Kupriyanov M Y 2003 *Pis'ma Zh. Eksp. Teor. Fiz.* **77** 609
Fominov Y V, Golubov A A and Kupriyanov M Y 2003 *JETP Lett.* **77** 510 (Engl. transl.)
- [28] Fominov Y V, Golubov A A, Karminskaya T Y, Kupriyanov M Y, Deminov R G and Tagirov L R 2010 *Pis'ma Zh. Eksp. Teor. Fiz.* **91** 329
Fominov Y V, Golubov A A, Karminskaya T Y, Kupriyanov M Y, Deminov R G and Tagirov L R 2010 *JETP Lett.* **91** 308 (Engl. transl.)
- [29] Vasenko A S, Ozaeta A, Kawabata S, Hekking F W J and Bergeret F S 2013 *J. Supercond. Novel Magn.* **26** 1951
- [30] Meng H, Wu X, Zheng Z and Xing D Y 2013 Long-range triplet Josephson current modulated by the interface magnetization texture *Europhys. Lett.* **104** 37003
- [31] Kawabata S, Asano Y, Tanaka Y and Golubov A A 2013 *J. Phys. Soc. Japan* **82** 124702
- [32] Ryazanov V V, Oboznov V A, Rusanov A Y, Veretennikov A V, Golubov A A and Aarts J 2001 *Phys. Rev. Lett.* **86** 2427
- [33] Oboznov V A, Bol'ginov V V, Feofanov A K, Ryazanov V V and Buzdin A I 2006 *Phys. Rev. Lett.* **96** 197003
- [34] Kontos T *et al* 2002 *Phys. Rev. Lett.* **89** 137007
- [35] Sellier H, Baraduc C, Lefloch F and Calemczuck R 2003 *Phys. Rev. B* **68** 054531
- [36] Blum Y *et al* 2004 *Phys. Rev. B* **70** 214501
- [37] Bell C, Loloee R, Burnell G and Blamire M G 2005 *Phys. Rev. B* **71** 180501(R)
- [38] Weides M, Kemmler M, Kohlstedt H, Buzdin A I, Goldobin E, Koelle D and Kleiner R 2006 *Appl. Phys. Lett.* **89** 122511
- [39] Pfeiffer J, Kemmler M, Koelle D, Kleiner R, Goldobin E, Weides M, Feofanov A K, Lisenfeld J and Ustinov A V 2008 *Phys. Rev. B* **77** 214506
- [40] Sosnin I, Cho H, Petrashov V T and Volkov A F 2006 *Phys. Rev. Lett.* **96** 157002
- [41] Keizer R S, Goennenwein S T B, Klapwijk T M, Miao G, Xiao G and Gupta A 2006 *Nature* **439** 825
- [42] Robinson J W A, Witt J D S and Blamire M G 2010 *Science* **329** 59
- [43] Sprungmann D, Westerholt K, Zabel H, Weides M and Kohlstedt H 2010 *Phys. Rev. B* **82** 060505(R)
- [44] Wang J, Singh M, Tian M, Kumar N, Liu B, Shi C, Jain J K, Samarth N, Mallouk T E and Chan M H W 2010 *Nat. Phys.* **6** 389
- [45] Anwar M S, Czeschka F, Hesselberth M, Porcu M and Aarts J 2010 *Phys. Rev. B* **82** 100501(R)
- [46] Anwar M S and Aarts J 2011 *Supercond. Sci. Technol.* **24** 024016
- [47] Anwar M S, Veldhorst M, Brinkman A and Aarts J 2012 *Appl. Phys. Lett.* **100** 052602
- [48] Khaire T S, Khasawneh M A, Pratt W P Jr and Birge N O 2010 *Phys. Rev. Lett.* **104** 137002
- [49] Khasawneh M A, Khaire T S, Klose C, Pratt W P Jr and Birge N O 2011 *Supercond. Sci. Technol.* **24** 024005
- [50] Klose C *et al* 2012 *Phys. Rev. Lett.* **108** 127002
- [51] Leksins P V, Garif'yanov N N, Garifullin I A, Schumann J, Kataev V, Schmidt O G and Buehner B 2011 *Phys. Rev. Lett.* **106** 067005
- [52] Zdravkov V I *et al* 2013 *Phys. Rev. B* **87** 144507
- [53] Herr A, Naaman O, Miller D and Herr Q 2012 Josephson Magnetic Random Access Memory (JMRAM) *Conference Program Book of 2012 Applied Superconductivity Conference* October 7–12 (Portland, Oregon) p 608
- [54] Newman N, Herr A, Rowell J M, Rizzo N, Qader M, Singh R K, Ofer Naaman O and Miller D 2012 Materials and processing requirements for Josephson MRAM (JMRAM) devices for superconductor memory applications *Conference Program Book of 2012 Applied Superconductivity Conference* October 7–12 (Portland, Oregon) p 965
- [55] Holmes D S, Ripple A L and Manheimer M A 2013 *IEEE Trans. Appl. Supercond.* **23** 1701610

- [56] Ryazanov V V, Bol'ginov V V, Sobanin D S, Vernik I V, Tolpygo S K, Kadin A M and Mukhanov O A 2012 *Physics Procedia* **36** 35
- [57] Larkin T I, Bol'ginov V V, Stolyarov V S, Ryazanov V V, Vernik I V, Tolpygo S K and Mukhanov O A 2012 *Appl. Phys. Lett.* **100** 222601
- [58] Vernik I V, Bol'ginov V V, Bakurskiy S V, Golubov A A, Yu Kupriyanov M, Ryazanov V V and Mukhanov O A 2013 *IEEE Trans. Appl. Supercond.* **23** 1701208
- [59] Bakurskiy S V, Klenov N V, Soloviev I I, Bol'ginov V V, Ryazanov V V, Vernik I I, Mukhanov O A, Kupriyanov M Y and Golubov A A 2013 *Appl. Phys. Lett.* **102** 192603
- [60] Bakurskiy S V, Klenov N V, Soloviev I I, Kupriyanov M Y and Golubov A A 2013 *Phys. Rev. B* **88** 144519
- [61] Volkov A F, Zaitsev A V and Klapwijk T M 1993 *Physica C* **210** 21
- [62] Nazarov Y V and Stoof T H 1996 *Phys. Rev. Lett.* **76** 823
Nazarov Y V and Stoof T H 1996 *Phys. Rev. B* **53** 14496
- [63] Golubov A A, Wilhelm F K and Zaikin A D 1997 *Phys. Rev. B* **55** 1123
- [64] Belzig W, Wilhelm F K, Bruder C, Schoen G and Zaikin A D 1999 *Superlattices Microstruct.* **25** 1251
- [65] Asano Y, Tanaka Y, Golubov A A and Kashiwaya S 2007 *Phys. Rev. Lett.* **99** 067005

Библиотека БГУИР